applied sciences

MDPI

Article

Predeployment of Transponders for Dynamic Lightpath Provisioning in Translucent Spectrally–Spatially Flexible Optical Networks

Krzysztof Walkowiak [1,*], Mirosław Klinkowski [2], Adam Włodarczyk [1] and Andrzej Kasprzak [1]

1 Department of Systems and Computer Networks, Wroclaw University of Science and Technology, Wybrzeze Wyspianskiego 27, 50-370 Wroclaw, Poland; adam.wlodarczyk@pwr.edu.pl (A.W.); andrzej.kasprzak@pwr.edu.pl (A.K.)

2 National Institute of Telecommunications, 1 Szachowa Street, 04-894 Warsaw, Poland; M.Klinkowski@il-pib.pl

* Correspondence: krzysztof.walkowiak@pwr.edu.pl; Tel.: +48-71-320-33-61

Received: 17 March 2020; Accepted: 14 April 2020; Published: 17 April 2020

Abstract: We consider a dynamic lightpath provisioning problem in translucent spectrally–spatially flexible optical networks (SS-FONs) in which flexible signal regeneration is achieved with transponders operating in back-to-back (B2B) configurations. In the analyzed scenario, an important aspect that has a significant impact on the network performance is the decision on placement of transponders that can be used for two purposes: transmitting/receiving (add/drop) of optical signals at the source/destination nodes and regeneration of the signals at some intermediate nodes. We propose a new algorithm called scaled average used regenerators (SAUR). The key idea of the SAUR method is based on a data analytics approach, i.e., the algorithm exploits information on network traffic characteristics and the applied dynamic routing algorithm to obtain additional knowledge for the decision on transponder placement. The numerical results obtained for two representative topologies highlight that the proposed SAUR method outperforms reference algorithms in terms of the amount of traffic that can be accepted in the network. In other words, placement of transponders yielded by the SAUR method allows to increase the SS-FON throughput using only the existing resources, i.e., the network operator does not have to invest in new devices or fibers.

Keywords: dynamic routing; elastic optical network; lightpath regeneration; network optimization; space division multiplexing; transponder predeployment; translucent networks

1. Introduction

One of the main goals and challenges for telecoms and backbone optical networks operators is to provide high network throughput (amount of served traffic) in a cost-effective way. In recent years, we have been observing an evolution of optical networks from fixed-grid *wavelength division multiplexing* (WDM) networks to flex-grid spectrally flexible *elastic optical networks* (EONs) which allow for adaptive use of different modulation formats and multi-carrier (super-channel) transmission. Another possible step towards providing higher network throughput is using a *space division multiplexing* (SDM) paradigm—a relatively new optical network idea that extends the capacity and capabilities of optical networks. In particular, SDM enables parallel transmissions of a number of co-propagating spatial modes in appropriately designed optical fibers. *Spectrally–spatially flexible optical networks* (SS-FONs), which join the main features of SDM and EONs, provide numerous advantages such as substantial growth of transmission capacity, cost savings due to the use of integrated devices, and extended flexibility in resource management due to the introduction of the spatial domain (spatial modes) [1–3].

Another concept that has the capability to allow increasing network throughput are *translucent networks*. The key motivation behind translucent networks is to mitigate the limited transmission reach in optical networks by using signal regeneration to re-amplify, reshape, and retime the optical signals. Translucent optical networks are planned to account for limited transmission reach and deal with this issue by regenerating signals in selected nodes. Such networks enable a compromise between network design cost and service provisioning performance including network capacity. However, the regenerator placement becomes one of the main problems to be addressed when planning and operating the translucent networks [4].

The idea of translucent networks emerged in the context of WDM optical networks, and the key design challenge in such networks is to select regeneration nodes that allow for regeneration of WDM lightpaths. The arrival of EONs triggered a new research effort in the context of translucent networks because of the introduction of flexible frequency grids and the possibility to apply different modulation formats of different spectral efficiency and transmission reaches. In particular, in the case when the transmission distance of a particular lightpath exceeds the transmission reach of the applied modulation format, it is required to regenerate the signal. It should be mentioned that modulation formats offer a trade-off between the spectral efficiency and transmission reach, i.e., more spectrally efficient modulation formats provide shorter transmission reaches, but, at the same time, they require less spectrum resources [5].

In this work, for regeneration, we used an approach based on the application of transponders (TRXs) operating in back-to-back (B2B) configurations, i.e., with interconnections at the client side [6–10]. The main benefit of B2B regeneration is the fact that dedicated regenerators are not required. The optical network can be equipped only with tunable transponders that are utilized for two purposes: transmitting/receiving of the signal at the source/destination nodes (add/drop) and regeneration of the signal at some intermediate nodes. Therefore, semi-transparent (translucent) lightpath connections are established in optical networks with B2B regeneration. Moreover, according to Reference [10], the advent of elastic optical transponders allows to change the output signal modulation format during the regeneration process. This can be achieved by means of patch-cords or electronic cross-connects providing traffic interchange among several transponders. In consequence, the lightpath may consist of several transparent segments, where each segment uses a different modulation format. This leads to potentially lower consumption of spectrum and transponders resources and thus allows to allocate more traffic in the network and increase the network capacity.

According to our previous results presented in References [8,11], full flexibility in the B2B regeneration, which means the possibility of regeneration with modulation conversion in each node traversed by a lightpath, can significantly increase the amount of served traffic in the network and thus provide higher network throughput without the need to upgrade the network by adding new fibers. Nevertheless, using the B2B regeneration complicates the network operation and optimization, since the basic optimization problem in SS-FONs (i.e., routing, spatial mode, and spectrum allocation (RSSA)) must be extended to account for allocation of transponders to lightpaths as well as for the fact that various nodes can be selected for regeneration.

Another important aspect that may also have a large impact on the network throughput in the context of translucent networks with B2B regeneration is transponder placement (i.e., predeployment) which is a new—when compared to classic regenerators placement—optimization problem that appears here. As mentioned above, the key aspect of the B2B regeneration is the fact that transponders are used for two goals: transmitting/receiving (add/drop) of the signal at the source/destination nodes and regeneration of the signal at some intermediate nodes. In consequence, the placement of transponders must address these two potential usage scenarios of transponders, as the lack of free transponders can be the reason of request blocking when there are not enough devices to transmit, receive or regenerate optical signals. The previous works focused on regenerator placement have accounted only for the optical signal regeneration scenario, while the transponders used to transmit/receive the signal have been assumed to be unlimited in the network, and thus the transponder placement has not been

addressed. Moreover, legacy regenerators receive a signal at a given data rate and, after regeneration, retransmit it with the same modulation format.

To the best of our knowledge, the only paper that concerns the transponder placement problem in SS-FONs with B2B regeneration is our work [12] that presents some initial research in this topic. In this paper, as the main novelty and contribution, we present a new algorithm for transponder predeployment in SS-FONs with B2B regeneration. The reported results obtained by means of extensive simulation experiments, run on two representative network topologies with realistic assumptions, clearly show that our method outperforms other reference methods. Moreover, according to the recent trends in optical networking, in this paper we consider a data analytics approach assuming that the proposed algorithm is traffic and routing aware. We assume that based on historical data on network traffic or traffic prediction methods, we know the key characteristics of the traffic, which can be next used as an input to dynamic routing simulations. By these means, we can observe the network performance and collect various data that then are applied to improve network performance. To verify this approach, we ran experiments for five various traffic profiles, while the overwhelming majority of previous papers focusing on optimization of dynamic optical networks have assumed only one traffic profile based on uniform distribution of communicating nodes. In consequence, we provide a study showing how the network traffic characteristics influence performance of the algorithms and the general performance of the SS-FON.

The rest of the paper is organized in the following way. In Section 2, we discuss related works. In Section 3, we describe the considered network and lightpath regeneration scenarios. In Section 4, we develop a transponder predeployment algorithm. In Section 5, we evaluate the algorithm performance with reference to other methods and analyze various network scenarios. Finally, Section 6 concludes the whole work.

2. Related Works

The basic optimization problem related to the design of translucent optical networks is regenerator placement (RPL). The RPL problem consists of selecting regeneration nodes in the network and deciding on the number of regenerators that should be installed in each of these nodes. This problem is addressed under the consideration of the transmission reach in optical networks. An optical signal can only travel a maximum distance before its quality deteriorates to the point that it must be regenerated using an installed regenerator. As the regenerator cost is high, the objective is to deploy in the network as few regenerators as possible while ensuring all nodes can communicate with each other [4,13].

In Reference [14], four regenerator placement algorithms were proposed: two of them were topology based (i.e., information on the network topology is utilized in the algorithms), and two methods were traffic prediction based (i.e., certain information about foreseen network traffic is available). The problem of network planning with routing and wavelength assignment (RWA) and RPL for a set of static traffic demands was studied in translucent WDM networks in Reference [15]. Moreover, various RWA methods were verified together with the RPL methods in order to find the best combination of RPL and RWA methods guaranteeing the lowest blocking probability. The authors of Reference [13] showed that the RLP is NP-Complete and developed three heuristics for the RLP based on various graph theory approaches. In Reference [16], analytical results showing the complexity of the RPL problem were presented. Four cases were considered with an upper bound on the number of regenerators installed at each node and where information on routing and/or information on the requests were given. The authors of Reference [17] proposed two new strategies for sparse regenerator placement in translucent optical networks, named most-used regenerator placement (MU-RP) and most-simultaneous-used regenerator placement (MSU-RP). Both proposed methods are based on preliminary simulations of the network to obtain statistics on regenerator usage, which are next applied for regenerator placement. The reported results showed that the MSU-RP algorithm outperformed all previous approaches. In Reference [18], four strategies for regenerator predeployment in WDM

network were presented, starting with a basic uniform distribution of regenerators followed by three topology-based methods that can be enriched with information on network traffic.

However, it should be underlined that all of the abovementioned papers were focused on fixed-grid WDM networks. Now, we briefly discuss previous research on regenerator placement in EONs. In Reference [19] in which the spectrum allocation and regenerator placement problem was considered, a heuristic method was proposed for a static optimization scenario. The reported results showed that use of regenerators considerably decreases the utilization of spectrum resources in a translucent EON. The authors of Reference [20] addressed jointly power management and regenerator placement in mixed line rate (MLR) optical networks, and they formulated an integer linear program for the regenerator placement problem. The authors of Reference [7] proposed a dynamic algorithm for energy-efficient routing and spectrum assignment in EONs with regenerator placement. The algorithm is based on a virtual graph, and the cost is computed according to the energy consumption of the corresponding links and intermediates routers. In Reference [21], four algorithms of regenerator placement for cloud-ready EONs were described. Two of the proposed methods utilize additional knowledge of data center location and these methods provide better performance results than simpler approaches. The author of Reference [22] described an approach for regenerator placement, routing, modulation level selection, and spectrum allocation in translucent EONs. For regenerator placement, an iterative method was proposed, where at each iteration a new regenerator site is added to a set of preset regenerator sites obtained in previous iterations, and the model is solved repeatedly for the remaining candidate locations. In Reference [23], a new regenerator allocation algorithm CIRA (circuit invigorating regenerators assignment) was proposed. The CIRA method accounts for quality of transmission (QoT) requirements. In more detail, the algorithm chooses the regenerators to be allocated in the network to reduce the effect of the physical layer and to minimize the QoT blocking. This is achieved by selecting more resistant signal modulation formats, when it is available. In the end, it leads to better overall performance (lower blocking ratio). Four different placement algorithms, namely, MSU, MU, NDF (node degree first), and DA (distance adaptive) were analyzed in the simulations, and the MSU provided the best results. The authors of Reference [24] developed and evaluated an auxiliary-graph-based approach for regenerator assignment in translucent elastic optical networks. The proposed method allows to analyze each possible transparent segment in the considered route. A special cost function was defined for each edge of the auxiliary graph representing a single segment that allows to apply a standard routing algorithm to find a path in the considered auxiliary graph. Several edge cost functions were examined. For regeneration placement, the NDF method was applied. Finally, in Reference [25], the problem of regenerator assignment in dynamic translucent optical networks was examined. It was assumed that each lightpath could be divided into several transparent segments, connected by 3R regenerators capable of accomplishing modulation format and spectrum conversion. It was assumed that the regenerators were placed uniformly in the network, i.e., each node had the same number of regenerators.

All the above discussed works are focused on various aspects related to the classic regenerator placement problem. However, we should stress that in this paper—due to the use of the B2B regeneration—instead of the elementary regenerator placement problem, a more broad problem of transponder placement (predeployment) is considered, where the transponders are used flexibly either for signal transmission/reception (add/drop) or signal regeneration purposes. As discussed below in the paper, a proper placement of transponders can significantly increase the amount of network traffic served in the network without any additional capital expenditures, since only the existing resources available in the network are utilized. Therefore, in our opinion, the problem addressed in this paper is of significant importance for network operators. The considered problem is relatively new, and the only paper that addresses the problem of transponders placement in optical networks with B2B regeneration is our work [12], where we presented preliminary research in this area. In particular, in Reference [12], we proposed several simple heuristic algorithms and compared their performance using a US topology. In this work, we continued our research on this problem, namely, we propose

a more advanced algorithm based on a data analytics approach and report the results of extensive simulations performed on two representative topologies with deep and insightful discussion of the obtained results.

Moreover, we want to mention that we have been working for the last few years on different types of RSA (routing and spectrum allocations) and RSSA problems in EONs and SS-FONs with B2B regeneration (e.g., [8,11]). However, all our previous papers that concerned B2B regeneration—except Reference [12]—do not address the problem of transponder placement.

3. Network Model

To model the SS-FON, we used a graph $G = (V, E)$, where V is a set of optical nodes, and E is a set of fiber links. Let set K include spatial modes available in each link $e \in E$. In each spatial mode $k \in K$, the available optical frequency spectrum is divided into frequency slices denoted as $S = \{s_1, s_2, \ldots, s_{|S|}\}$. We assume that each slice is of 12.5 GHz width. The transmission of optical signals is provided by means of spectral super-channels (SChs). A SCh can contain a number of optical carriers (OCs), each using Δ_{OC} frequency slices, where an OC is transmitted/received by one transponder. As proposed in [26] and [27], we assume that $\Delta_{OC} = 3$ slices, what is equivalent to 37.5 GHz. A set of modulation formats $M = \{m_1, \ldots, m_{|M|}\}$ is defined. Each modulation format $m \in M$ is characterized by a certain transmission reach and spectral efficiency. Moreover, modulation format $m \in M$ can support bit rate $g(m)$ on a single optical carrier.

In this paper, we considered a dynamic routing scenario assuming that a node-to-node dynamic traffic request d with a certain bit rate volume $h(d)$ is to be served in the network using a provisioned lightpath connection. For each request d, set $P(d)$ contains candidate routing paths generated using the k-shortest path algorithm. Each path $p \in P(d)$ connects the request source node and destination nodes and traverses intermediate nodes included in set $V(p) \subseteq V$. Each of intermediate nodes included in $V(p)$ can be selected as a regeneration point. As mentioned above, for regeneration we apply transponders operating in B2B configurations (i.e., with interconnections at the client side) [6,7]. Figure 1 illustrates the general idea of the B2B regeneration. For more information on the SS-FON with B2B regeneration network model refer to Reference [11].

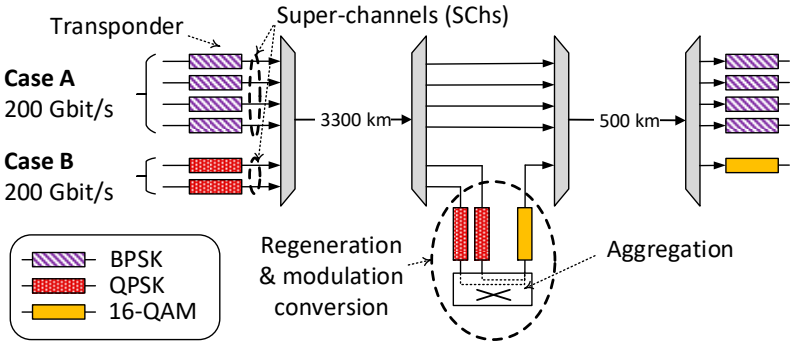

Figure 1. Provisioning of a 200 Gbit/s lightpath without back-to-back (B2B) regeneration (case A) and with B2B regeneration (case B). The following modulation formats are applied: BPSK (Binary Phase Shift Keying), QPSK (Quadrature Phase Shift Keying), and 16-QAM (Quadrature Amplitude Modulation).

In our previous papers, we examined three B2B regeneration scenarios: minimal regeneration, regeneration without modulation conversion, and flexible regeneration allowing for modulation conversion. Since, according to the results presented in References [11,25,28], the flexible approach provides the best results in terms of blocking probability, in this paper we focused only on this scenario. In the flexible B2B regeneration, a full flexibility of the B2B regeneration was assumed [29]. In more detail, an extra regeneration of SChs with modulation conversion can be applied in any intermediate node of the routing path. The motivation behind full flexibility is to use more efficient modulation formats for shorter transparent path segments with the possibility to apply different modulation

formats on different segments, i.e., modulation conversion and spectrum conversion is allowed in regeneration nodes. Nevertheless, the flexible regeneration, apart from switching the regenerated data units, may require to (dis)aggregate them in order to match the capacity of transponders operating with different modulation formats. It should be stressed that the presented model can be easily adapted to other assumptions that described above, e.g., different values of Δ_{OC}.

To illustrate the considered B2B regeneration approach and the effect of transponder placement, we consider a simple example shown in Figure 2. We assume four modulation formats, namely, BPSK, QPSK, 8-QAM, and 16-QAM, with the bit rates transmitted by OCs and the transmission reaches of considered modulation formats based on data presented in [26] and [27] and shown in Table 1. A request (lightpath) is allocated on a routing path (a, b, c, d) of an overall length 3800 km consisting of three links: (a, b) 1000 km, (b, c) 2300 km, and (c, d) 500 km. Moreover, every link (i.e., (a, b), (b, c), (c, d)) has 12 free adjacent slices available that can be used to allocate the request. Twenty transponders are available in the network to be located in nodes a, b, c, and d using various predeployment policies. We consider the following four scenarios of transponder location:

- {5, 5, 5, 5}, i.e., every node has 5 transponders, and the lightpath uses transponders in the following way <2, 5, 5, 2> (Figure 2a);
- {10, 0, 0, 10}, i.e., 10 transponders are placed in nodes a and d, and the lightpath uses transponders in the following way <4, 0, 0, 4> (Figure 2b);
- {8, 0, 8, 4}, i.e., 8 transponders are placed in nodes a and c, 4 transponders are placed in node d, and the lightpath uses transponders in the following way <4, 0, 6, 2> (Figure 2c);
- {3, 7, 7, 3}, i.e., 3 transponders are placed in nodes a and d, 7 transponders are placed in nodes b and c, and the lightpath uses transponders in the following way <3, 7, 7, 2> (Figure 2d).

Note that the numbers in curly brackets { } represent the number of transponders located in each network node that can be used for establishing the considered lightpath. However, some of these transponders can remain non-allocated, and numbers in angle brackets < > and Figure 2 show only the transponders that are used to establish the considered lightpath, i.e., other spare transponders are not presented in the figure.

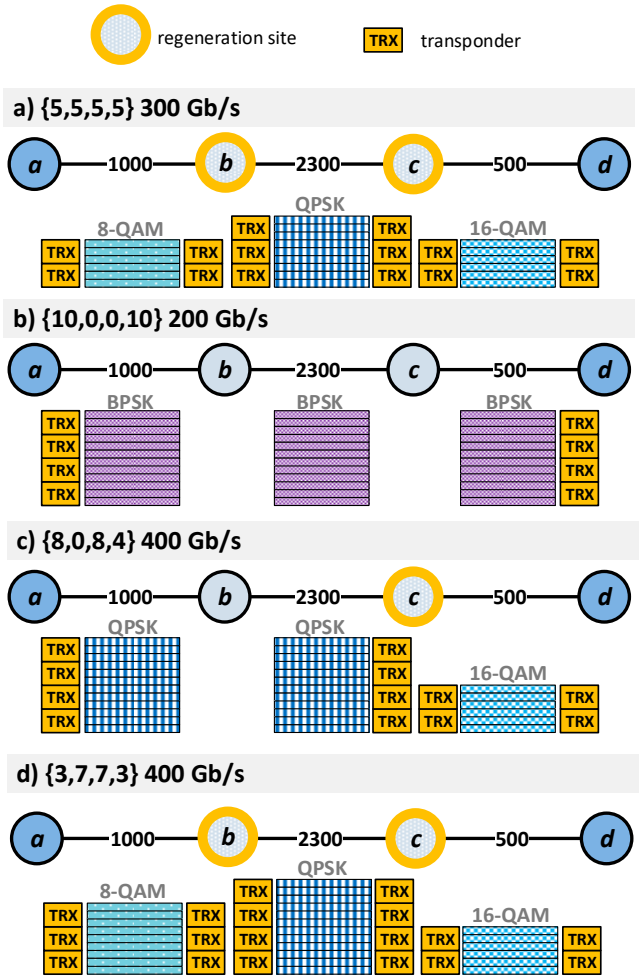

Figure 2. Example of different transponder placement scenarios for provisioning a request: a) placement of transponders in network nodes: {5, 5, 5, 5}; b) placement of transponders in network nodes: {10, 0, 0, 10}; c) placement of transponders in network nodes: {8, 0, 8, 4}; d) placement of transponders in network nodes: {3, 7, 7, 3}.

Table 1. Transmission reaches (km) and supported bit rates (Gb/s) per one transponder for considered modulation formats.

Modulation Format	Reach (km)	Bit Rate Supported by One Transponder (Gb/s)
BPSK	6300	50
QPSK	3500	100
8-QAM	1200	150
16-QAM	600	200

For each of transponder placement scenarios, the request can be established using different regeneration options (configurations), where each option divides the transmission path into a number of transparent path segments. For each segment, we select the best allowable modulation format. The objective is to provision the request with the highest possible bit rate (throughput) accounting for limited resources of spectrum (12 adjacent slices) and transponders (20 devices located in various scenarios). We assume the flexible B2B regeneration approach. We can easily observe that the placement of transponders has a significant impact on the allowable bit rate of the considered request, since the following bit rates are achieved for the considered four scenarios: (a) 300 Gb/s, (b) 200 Gb/s, (c) 400 Gb/s, (d) 400 Gb/s. From the above example, we can notice that in spectrally flexible optical networks, such as EONs and SS-FONs with B2B regeneration, the placement of transponders is a key issue, since by

proper predeployment of transponders one can allow to establish lightpaths with higher bit rate and thus serve more traffic without the need to deploy extra fibers.

4. Algorithms

In this section, we describe several algorithms developed for predeployment of transponders in SS-FONs with B2B regeneration. First, we present reference methods, mostly based on simple greedy algorithms. Next, we propose a new method scaled average used regenerators (SAUR) based on a data analytics approach. Let us assume that we are given T transponders to be located in network nodes in order to allow provisioning of the requests (lightpaths) with the possibility to use the B2B regeneration in some intermediate nodes of the routing path. Moreover, let $t(v)$ denote the number of transponders predeployed in node $v \in V$.

The basic approach proposed in our previous paper [12] assumes that the transponders are located in the network nodes proportionally to a selected metric. The following versions of this approach are considered in this paper.

Uniform location (UNI) assumes that each node is assigned with the same number of transponders [18]:

$$t(v)^{\mathrm{UNI}} = \lfloor T/|V| \rfloor. \tag{1}$$

Nodal degree (ND) assumes that transponders are located proportionally to the degree of network node [18]:

$$t(v)^{\mathrm{ND}} = \lfloor T \cdot nd(v) / \sum\nolimits_{w \in V} nd(w) \rfloor, \tag{2}$$

where $nd(v)$ denotes the node degree of node v.

Routing only (RO) assumes that transponders are located proportionally to the number of times a particular node is included in the shortest path considering all node pairs [18]:

$$t(v)^{\mathrm{RO}} = \lfloor T \cdot nsp(v) / \sum\nolimits_{w \in V} nsp(w) \rfloor, \tag{3}$$

where $nsp(v)$ denotes the number of times node v is included in the shortest path between a node pair considering all node pairs.

Configurations only (CONF) works similarly to RO; however, here, all the possible configurations (regeneration options) for the shortest path for each node pair are analyzed, and transponders are located proportionally to the number of times a particular node is included in the configuration considering all node pairs [12]:

$$t(v)^{\mathrm{CONF}} = \lfloor T \cdot ncsp(v) / \sum\nolimits_{w \in V} ncsp(w) \rfloor, \tag{4}$$

where $ncsp(v)$ denotes the number of times node v is included in a configuration based on the shortest path between a node pair considering all node pairs [12].

Combined (COMB) assumes that transponders are located according to a metric that includes three elements: nodal degree (weight 40%, proportionally), number of transponders in the end nodes in the best configuration according to a metric showing usage of network resources (weight 40%, proportionally), and average distance to other nodes (weight 20%, inversely proportionally) [12]:

$$t(v)^{\mathrm{COMB}} = \lfloor 0.4 \cdot t^{\mathrm{ND}}(v) + 0.4 \cdot t^{\mathrm{ENC}}(v) + 0.2 \cdot t^{\mathrm{AD}}(v) \rfloor, \tag{5}$$

where $t^{\mathrm{ND}}(v) = \lfloor T \cdot nd(v) / \sum_{w \in V} nd(w) \rfloor$ denotes the number of transponders assigned to node v according to nodal degree, $t^{\mathrm{ENC}}(v) = \lfloor T \cdot enc(v) / \sum_{w \in V} enc(w) \rfloor$ denotes the number of transponders assigned to node v according to number of transponders in the end nodes in the best configuration, and $t^{\mathrm{AD}}(v) = \lfloor (T \cdot (1/ad(v)) / \sum_{w \in V} (1/ad(w)) \rfloor$ denotes the number of transponders assigned to node v according to number of transponders in the end nodes in the best configuration.

It should be noted that the above presented algorithms do not account for additional knowledge that can be obtained by a data analytics approach which provides information on the network traffic profile observed in the near past or predicted for the future. Now, we present two traffic-based methods. In both proposed methods, for solving the dynamic RSSA problem we use the adaptive routing with back-to-back regeneration (ARBR) algorithm proposed in our previous paper [11]. Note that the results from Reference [11] clearly confirm that the ARBR method provides much better results in terms of bandwidth blocking probability when compared to other methods in the context of SS-FONs with B2B regeneration.

The key element of the ARBR algorithm is that it accounts for two types of important resources in optical networks, namely, spectrum and transponders. In a nutshell, the ARBR is a highly adaptive routing algorithm that utilizes the key benefits of B2B regeneration. In the preprocessing phase of ARBR, using k shortest paths, a set of configurations defined by routing paths and location of regeneration points are computed for each node pair. For each transparent segment of a particular configuration, the most spectrally efficient modulation format is selected that supports transmission reach larger than the length of the considered segment. For each new request that occurs in the network, the ARBR algorithm executes the following procedure. Given the set of pre-computed configurations, a special adaptive metric is calculated for each configuration. This metric contains two elements: (i) static usage of spectrum (i.e., the number of slices essential to provision the considered configuration for a particular request) and transponders (i.e., the number of transponders essential to provision the considered configuration for a particular request); and (ii) dynamic usage of the spectrum and transponders resources (i.e., cost of the configuration that represents the current utilization of spectrum and transponders resources). Both elements (i.e., static and dynamic) are weighted with parameter α. Next, the configurations are processed in increasing order of the obtained configuration's metric. The ARBR tries to provision the request on the currently analyzed configuration, namely, using the first-fit approach, the algorithm searches for a sufficient range of spectrum checking various spatial modes. If the analyzed configuration is feasible, the request is provisioned in the network using this configuration. Otherwise, if none of the configurations is feasible, the request is rejected. To summarize, ARBR is able to analyze different configurations of routing paths and regeneration points to select the best option that balances between two key resources in the network, namely, spectrum resources (slices) and transponders. Moreover, the ARBR algorithm can adapt to the dynamically changing conditions in the network by selecting routing paths and regeneration points according to the current utilization of spectrum and transponders resources. For more details on ARBR, the reader is referred to Reference [11].

The first traffic-based transponder placement algorithm is MSU proposed in Reference [17] and adapted to our problem. In particular, MSU distributes T transponders over the network based on the maximum instantaneous number of transponders used in each node during the simulation of the dynamic routing simulation with the use of the ARBR method. During the simulations, it was assumed that nodes were equipped with an unlimited number of transponders and the traffic is generated following a known (predicted) traffic pattern.

Finally, we present a novel SAUR algorithm. In Figure 3, we report the general workflow of this method, while Figure 4 shows the pseudocode. The idea of SAUR is to utilize knowledge on network traffic and allocation method in order to predeploy the transponders in such a way that the network performance in terms of bandwidth blocking probability is improved, or in other words, more traffic can be accepted in the network.

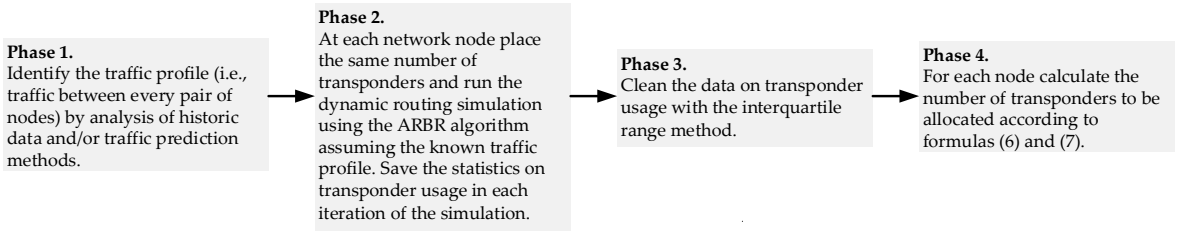

Figure 3. Workflow of the scaled average used regenerators (SAUR) method.

	Algorithm SAUR(β).
1	For each $v \in V$ place the same number of transponders, i.e., $t(v) \leftarrow \lfloor T / \lvert V \rvert \rfloor$.
2	Run simulation (dynamic traffic) using the ARBR algorithm considering all network nodes with $t(v)$ pre-deployed transponders assuming a known traffic profile and store the statistics on transponder usage in each iteration.
3	Clean the data on transponder usage with the interquartile range method.
4	For $v \in V$ calculate $avt(v)$ – the average usage of transponders over all iterations of the dynamic traffic simulation.
5	For each $v \in V$ calculate $a(v) \leftarrow power(avt(v), \beta)$.
6	For each $v \in V$ calculate $t(v)^{\text{SAUR}} \leftarrow \lfloor (a(v) \cdot T / \Sigma_{v \in V} a(v) \rfloor$.

Figure 4. SAUR pseudocode.

The key idea of SAUR is quite simple. First, each network node is assigned with the same number of transponders (Step 1), i.e., $t(v) = \lfloor T/|V| \rfloor$, which according to Reference [12] provides good results. Next, we run the ARBR dynamic routing algorithm described above to simulate the network operation assuming a randomly generated lightpath requests following a known (predicted) traffic pattern (Step 2). During simulation, various statistics on transponder usage in network nodes are collected. Since the traffic in the network is stochastic, therefore, to improve the quality of the obtained statistics of transponder usage, we perform data cleaning using the interquartile range method to remove outliers for each of analyzed nodes (Step 3). The interquartile range method is a measure of variability, based on dividing a rank-ordered data set into four equal parts (quartiles). The values that divide each part are denoted by Q1, Q2, and Q3. Interquartile range (IQR) is equal (Q3 – Q1), i.e., the difference between third and first quartiles. Outliers are defined as observations that fall below (Q1 − 1.5 IQR) or above (Q3 + 1.5 IQR). Next, for each node parameter, $avt(v)$ is obtained (Step 4). In more detail, $avt(v)$ denotes the average usage of transponders estimated over all time iterations. In particular, the time scale is divided into time slots (iterations) in which new requests arrive to the network and some other requests are finished according to the assumed average arrival rates and lifetimes. After each iteration, various statistics on the network usage are calculated, including usage of transponders at network nodes. To account for different traffic characteristics, in SAUR we use *scaled* allocation, i.e., transponders are allocated proportionally to the average usage scaled by using the power function with exponent β. To this end, in Step 5, parameter $a(v)$ is calculated using the following formula:

$$a(v) = power(avt(v), \beta), \tag{6}$$

Finally, in Step 6, the number of transponders assigned to each node is computed using $a(v)$:

$$t(v)^{\text{SAUR}} = \lfloor (a(v) \cdot T / \sum\nolimits_{w \in V} a(w) \rfloor, \tag{7}$$

As mentioned above, MSU and SAUR are both traffic-based approaches that use data obtained by simulation of the routing algorithm for a selected network profile. However, when compared to MSU, SAUR provides the following key differences. First, SAUR addresses the fact that in our

network model, B2B regeneration is allowed, i.e., we predeploy transponders that are used not only for regeneration of the signal at some intermediate nodes (as in MSU) but also for transmitting/receiving (add/drop) of the signal at the source/destination. Second, in our previous research on performance of SS-FONs with B2B regeneration, we noticed that, according to the number of available transponders in the network (parameter T), the performance of the network changes (for instance, see the results in References [11,12]). Therefore, we assume that every node has a limit of available transponders in the dynamic routing simulations, and thus there is the possibility of a lack of transponders at some network nodes which will affect the performance of the dynamic routing algorithm. In contrast, the MSU method assumes that during the simulations there are no limits on the number of regenerators available in the network nodes. Third, SAUR allocates transponders according to their average usage observed during the whole simulation, while MSU focuses on the maximum usage. This difference between both methods is motivated by the fact that, in our opinion, the average utilization observed over a longer period of time is more important than short-term dependencies that can occur due to the stochastic nature of the network traffic and dominate the final allocation of transponders. Finally, the proposed SAUR method can be tuned, i.e., transponders are allocated proportionally to the average usage scaled by using the power function with exponent β. In this way, we can adjust the performance of SAUR to account for different traffic profiles that can occur in the network.

It should be stressed that the two traffic-based methods described above (i.e., MSU and SAUR) strongly rely on the data analytics approach. Firstly, these methods depend on the knowledge on the network traffic obtained by analysis of historical data or traffic prediction methods. With this information, both methods can tune their performance to different traffic profiles which results in different decisions in terms of the transponder placement. Without the detailed knowledge on the traffic profile, usually a uniform traffic profile is assumed, which results in a particular placement of transponders which may not be the best for traffic profiles different than uniform. Secondly, both methods during their run (i.e., simulation of network routing over a period of time) collect data on transponder usage for each node in subsequent iterations of the considered time period which allows to find some statistics such as maximum usage (MSU) or average usage (SAUR). Next, these statistics are directly applied to make the final decision on transponder placement.

In terms of time complexity of the above described algorithms, the time complexity of the UNI and ND methods is simply $O(|V|)$, where $|V|$ denotes the number of nodes. In the case of RO, CONF, and COMB, the time complexity is dominated by the shortest path calculation and can be estimated as $O(|V|^3)$ assuming the Floyd–Warshall algorithm. Finally, the time complexity of the two last methods, MSU and SAUR, depend on the execution time of the ARBR algorithm and the size of network traffic to be simulated. However, the final placement of transponders has simple complexity of $O(|V|)$. Thus, the overall complexity of MSU and SAUR can be formulated as $O(|V| + time(\text{ARBR}))$, where $time(\text{ARBR})$ denotes the execution time required to simulate the analyzed traffic with the use of the ARBR method.

5. Results

5.1. Simulation Setup

We ran simulations for two realistic large network topologies: the European backbone network called Euro28 (28 nodes, 84 links, average link length of 625 km) and the US national network called US26 (26 nodes, 82 links, average link length of 755 km) [30]. Both topologies are shown in Figure 5. We assumed that each network link was a bundle of 7 SMFs (single-mode fibers) and each fiber offered 4 THz spectrum (320 slices of 12.5 GHz width each). The general assumptions on the SS-FON architecture were similar as in References [11,12]. In particular, we considered four modulation formats, namely, BPSK, QPSK, 8-QAM, and 16-QAM. Based on the data presented in References [26,27], we assumed that coherent transponders transmitted/received the signals of 3 slices (i.e., 37.5 GHz). The bit rates supported by a transponder depended on the applied modulation format and are presented in Table 1. In the case where the requested bit rate exceeded the transponder capacity using a particular

modulation format, the request was served within one spectral SCh allocated via an adequate number of adjacent slices. For instance, if the request bit rate was 300 Gb/s, using the QPSK modulation format, 3 transponders were required with a spectral SCh consisting of 9 slices. In turn, if the 8-QAM modulation format was selected, the same 300 Gb/s request would need 2 transponders with 6 slices. Each established SCh was separated from neighboring SChs by 1 slice (12.5 GHz) guard-band. The transmission reaches of the modulation formats were taken from References [27] and are reported in Table 1. However, we want to stress that the presented network model (Section 3) and algorithms (Section 4) are generic, and they can be easily adapted to other parameters describing the applied modulation formats.

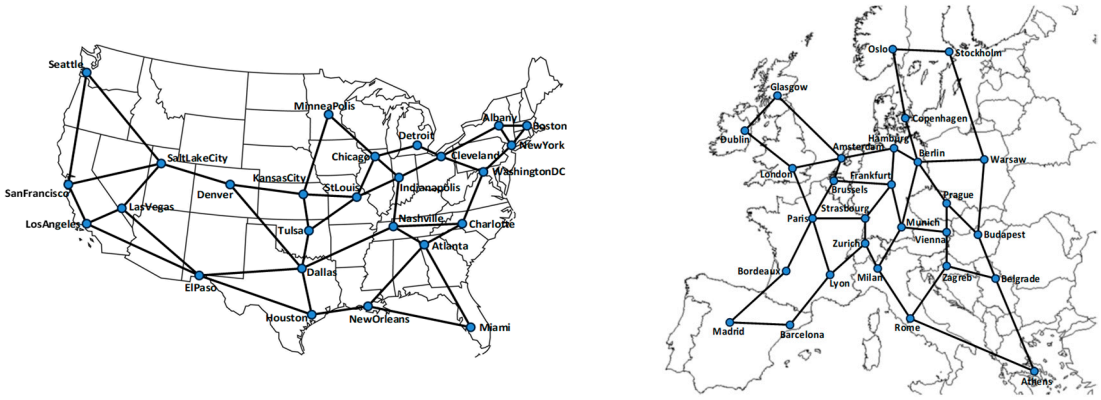

(**a**) (**b**)

Figure 5. Tested network topologies: US26 (**a**), Euro28 (**b**).

According to our previous experiments reported in Reference [11], the following three numbers of transponders that can be predeployed in the network have been selected for the simulations: 10,000; 15,000; and 20,000. It should be noted that in the considered SS-FON scenario, bandwidth blocking probability can occur due to the fact of two reasons: lack of spectrum resources or lack of transponders. The three selected numbers of transponders assure that we would be able to analyze the three different cases in the simulations: (i) the blocking was mostly due to the lack of transponders (budget of 10,000 transponders); the blocking was due to the lack of both transponders and spectrum (budget of 15,000 transponders); and (iii) the blocking was mostly due to the lack of spectrum (budget of 20,000 transponders).

For dynamic routing (i.e., establishing the arriving request in the network), we applied the ARBR algorithm proposed in Reference [11] with the tuning parameter $\alpha = 0.8$, according to the tuning process presented in Reference [11]. We use $k = 5$ shortest paths applied to generate candidate lightpaths including routing and regeneration configurations.

Traffic requests were generated randomly with bit rates from 50 Gb/s to 1 Tb/s, changing with a 50 Gb/s granularity. The requests arrived at the network according to a Poisson process with an average arrival rate of λ requests per time-unit. In turn, the lifetime of each request followed a negative exponential distribution with an average of $1/\mu$. Consequently, the offered total traffic load was λ/μ normalized traffic units (NTUs). As the average bit rate of a single request was 525 Gb/s, 100 NTUs corresponded to about 52.5 Tb/s of the offered traffic load. For each of the simulated traffic load given in NTUs, we generated a set of 60,000 requests; however, the first 5000 requests were not included in the analysis in order to allow the network to reach a stable condition.

Most of the previous works that examine dynamic routing in optical network considered only one traffic profile assuming uniform traffic distribution among all network nodes. In this paper, to make a more thorough investigation, we analyzed five traffic profiles (TPs) different in terms of the source–destination (s–d) nodes' distribution. The general idea of the traffic generation is based on the multivariable gravity model [31]. In more detail, the traffic generation is based on several components

which can be tuned according to considered scenarios. The source node selection probability is based on metrics describing the nodes (cities), such as population of the country/city and GDP of the country/city, based on data available in Wikipedia. In turn, the destination node selection probability is based on various functions of the distance between each nodes pair (e.g., square root). In consequence, the created traffic reflects the multivariable gravity model with different parameters to account for the fact that the traffic in contemporary networks is highly dependent on services such as cloud computing and edge computing.

The analyzed traffic profiles are as follows:

- TP A. The distribution of requests between s–d nodes is uniform, i.e., the source node selection probability is the same for all nodes and the same applies for every node to be chosen as the destination node.
- TP B. The distribution of requests between s–d nodes is inversely proportional to the square root of the distance between node pairs, i.e., the source node selection probability is uniform, but the probability of choosing the destination node is inversely proportional to the square root of the distance between selected source node and each of the remaining nodes.
- TP C. The distribution of requests between s–d nodes is inversely proportional to the distance between node pairs, i.e., the source node selection probability is uniform, but the probability of choosing the destination node is inversely proportional to the distance between selected source node and each of the remaining nodes.
- TP D. The distribution of requests between s–d nodes depends on the square root of two elements: distance between nodes (inversely) and product of population and GDP for given node, i.e., the source node selection probability is proportional to the square root of the product of population and GDP for given node. In turn, the probability of destination node selection is inversely proportional to the square root of the distance between chosen source node and each of the remaining nodes.
- TP E. The distribution of requests between s–d nodes depends on two elements: distance between nodes (inversely) and product of population and GDP for given node, i.e., the source node selection probability is proportional to the product of population and GDP for a given node. In turn, the probability of destination node selection is inversely proportional to the distance between chosen source node and each of the remaining nodes.

The basic performance metric used in the simulations is *bandwidth blocking probability* (BBP) defined as the volume of rejected traffic divided by the volume of whole traffic offered to the network. Moreover, we use a metric called *accepted traffic* which denotes the maximum traffic that can be provisioned in the network with BBP not greater than 1% which is a commonly acceptable threshold for BBP.

5.2. Tuning of the SAUR Algorithm

The first goal of simulations was to tune the SAUR algorithm. To recall, the SAUR method has one tuning parameter β that is used to scale the impact of average transponder usage on the placement of transponders in particular nodes. After some preliminary experiments, we decided to test the values of parameter β in the range from 0.0 to 2.0 with step 0.2. In Table 2, we present the results of the tuning process, i.e., values of parameter β providing the best results in terms of the accepted traffic for US26 and Euro28 networks. We should underline that the obtained values of parameter β are quite similar for both analyzed topologies.

Table 2. Tuning of the SAUR algorithm—values of the scaling parameter yielding the best result as a function of different number of transponders (TRXs) and various traffic profiles (TP)

Number of TRXs	US26 Network					Euro28 Network				
	TP A	TP B	TP C	TP D	TP E	TP A	TP B	TP C	TP D	TP E
10,000	1.4	1.4	1.0	1.2	1.0	1.4	1.4	1.0	1.0	0.8
15,000	1.6	1.4	1.2	1.2	1.0	2.0	1.4	1.0	1.2	1.2
20,000	2	1.4	1.0	1.4	0.8	2.0	1.8	1.4	1.6	0.8

In turn, in Figures 6 and 7 we present detailed results showing the performance of the SAUR method for the tested values of parameter β for networks US26 and Euro28, respectively, with 10,000 and 20,000 transponders available in the network. The key observation from these figures is that the impact of the tuning parameter was the largest for TP E, while for other traffic profiles the impact was smaller, especially for larger number of available transponders (i.e., 20,000). This follows from the fact that TP E had the largest variations in values of traffic bit rate between different node pairs, and thus the placement of transponders was very important for both transmitting/receiving (end nodes) and regeneration. It should be noted that in the following subsections, the reported results of the SAUR method were obtained using the values of the tuning parameter β shown in Table 2.

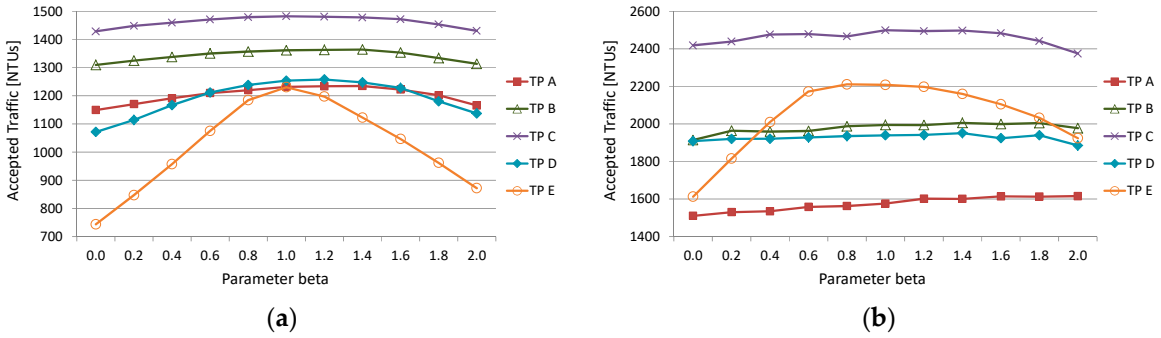

Figure 6. Tuning of the SAUR algorithm—accepted traffic as a function of tuning parameter β for the US26 network with different traffic profiles: (**a**) 10,000 transponders, (**b**) 20,000 transponders.

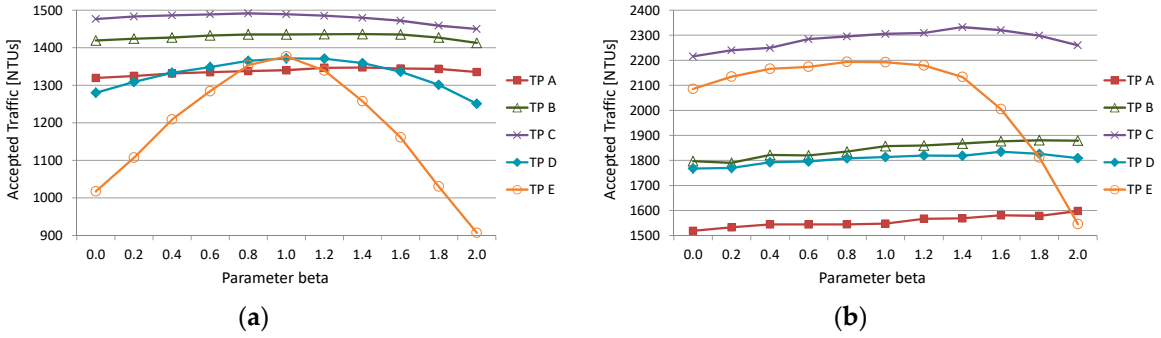

Figure 7. Tuning of the SAUR algorithm—accepted traffic as a function of tuning parameter β for the Euro28 network with different traffic profiles: (**a**) 10,000 transponders, (**b**) 20,000 transponders.

5.3. Comparison of Algorithms

The next goal of experiments was to compare the novel SAUR transponder placement algorithm against reference methods described in Section 4 and adapted to the considered problem, namely, UNI [18], ND [18], RO [18], CONF [12], COMB [12], and MSU [17]. In Table 3, we show the ranking of the tested methods for US26 and Euro28 networks in terms of the accepted traffic. Three values of the numbers of available transponders were considered: 10,000, 15,000, and 20,000. The same traffic profiles as in previous sections were analyzed. For each separate case (i.e., network topology and traffic

profile), the transponders were predeployed using a particular method. Next, we ran the dynamic routing ARBR algorithm to measure the amount of accepted traffic assuming the 1% of BBP. The best predeployment method received 1 point (first place), the second method received 2 points (second place), etc. Next, we averaged the ranking over all five tested traffic profiles for a particular number of transponders. We can easily notice that the SAUR method always provided the best results. The MSU, UNI, and COMB methods share places 2–4, and the position of each method depends on the analyzed scenarios (topology and number of transponders). The three remaining methods (ND, RO, and CONF) provided much worse results compared to the other methods. Therefore, for further detailed analysis, we used the four best algorithms, namely, UNI, COMB, MSU, and SAUR.

Table 3. Average ranking of algorithms for various number of transponders.

Network	**US26**			**Euro28**		
Number of TRX	**10,000**	**15,000**	**20,000**	**10,000**	**15,000**	**20,000**
UNI	2.6	3	4.2	2.2	3.6	4.8
ND	4.8	5	4.4	5	5	4
RO	7	7	7	7	7	7
CONF	6	6	6	6	6	5.4
COMB	2.8	2.6	3.2	3.2	2.8	3.8
MSU	3.8	3.4	2.2	3.6	2.6	2
SAUR	1	1	1	1	1	1

In Tables 4 and 5, we report detailed results obtained for UNI, COMB, MSU, and SAUR for US26 and Euro28 networks, respectively. We present two performance metrics: accepted traffic in NTUs and the percentage distance to the SAUR method. First of all, the results confirm the trends described above, in particular, in all cases the SAUR method is the best one, i.e., it allows to provision in the network the highest amount of traffic among all tested approaches. However, we can easily notice that the differences between examined methods strongly depend on the number of transponders and selected traffic profiles. In particular, with the increase of the available transponders, the gaps between SAUR and MSU decrease regardless of the traffic profile. In the case of UNI and COMB methods, this trend is not so regular. But—comparing the performance for different number of transponders—the smallest gaps between the analyzed methods are obtained for the largest number of 20,000 transponders. This trend can be explained by the fact that with larger number of transponders the placement of transponders effects the results (accepted traffic) to a smaller extent, since more transponders cause that the blocking occurs mostly due to the limited resources of optical spectrum and additional transponders (regardless of their placement) cannot help overcoming this problem.

Table 4. Comparison of algorithms for various number of transponders and traffic profiles, US26 network in terms of the accepted traffic expressed in NTUs (network traffic units).

TP	Accepted Traffic (NTUs)				Distance to SAUR		
	UNI	COMB	MSU	SAUR	UNI	COMB	MSU
			10,000 transponders				
A	1149	1178	927	1235	6.9%	4.6%	24.9%
B	1310	1322	1076	1364	4.0%	3.1%	21.2%
C	1429	1428	1242	1482	3.6%	3.7%	16.2%
D	1072	1041	968	1258	14.8%	17.2%	23.0%
E	744	732	968	1230	39.6%	40.5%	21.3%
			15,000 transponders				
A	1411	1451	1412	1559	9.6%	6.9%	9.5%
B	1738	1791	1715	1910	9.0%	6.3%	10.2%
C	2081	2158	1989	2226	6.5%	3.1%	10.7%
D	1636	1601	1517	1824	10.3%	12.2%	16.8%
E	1176	1165	1533	1875	37.3%	37.9%	18.2%
			20,000 transponders				
A	1511	1541	1585	1616	6.5%	4.7%	1.9%
B	1914	1941	1973	2006	4.6%	3.2%	1.7%
C	2418	2479	2487	2499	3.2%	0.8%	0.5%
D	1908	1926	1921	1951	2.2%	1.3%	1.6%
E	1613	1610	2088	2211	27.1%	27.2%	5.6%

Table 5. Comparison of algorithms for various number of transponders and traffic profiles, Euro28 network.

TP	Accepted Traffic [NTUs]				Distance to SAUR		
	UNI	COMB	MSU	SAUR	UNI	COMB	MSU
			10,000 transponders				
A	1319	1293	1075	1347	2.1%	4.0%	20.2%
B	1419	1377	1176	1436	1.2%	4.1%	18.1%
C	1476	1429	1222	1491	1.0%	4.2%	18.0%
D	1280	1180	1129	1371	6.7%	14.0%	17.7%
E	1017	910	1082	1377	26.1%	33.9%	21.4%
			15,000 transponders				
A	1500	1513	1526	1554	3.5%	2.6%	1.8%
B	1700	1756	1749	1807	5.9%	2.8%	3.2%
C	1994	2068	1917	2108	5.4%	1.9%	9.1%
D	1648	1678	1709	1780	7.4%	5.7%	4.0%
E	1619	1442	1754	1961	17.4%	26.4%	10.5%
			20,000 transponders				
A	1519	1540	1567	1598	4.9%	3.6%	1.9%
B	1797	1806	1874	1880	4.4%	3.9%	0.3%
C	2216	2248	2272	2332	5.0	3.6%	2.6%
D	1767	1792	1822	1834	3.6%	2.3%	0.7%
E	2085	1996	2173	2193	4.9%	9.0%	0.9%

Moreover, in Tables 4 and 5, we can see that the largest gaps between SAUR and other methods was obtained for the traffic profile E which again follows from the highest diversity of this traffic profile. Finally, the comparison of the tested network topologies shows that the gaps between SAUR and other methods were larger for the US26 network. This is due to the fact that US26 had on average larger distances between node pairs. In consequence, appropriate placement of transponders can provide

more benefits by allowing the regeneration in some network nodes which enables using more effective modulation formats than BPSK which allows to reduce the spectrum usage.

Furthermore, in Figures 8–10, we show the placement of predeployed transponders in the US26 network yielded by the UNI, COMB, MSU, and SAUR methods assuming three traffic profiles, namely, TP A, TP B, and TP C. Each figure presents the percentage of all available transponders assigned to each node (city) assuming various number of available transponders. The results of the UNI method are pointed out as a red line with value 3.85%, since in this method each of 26 nodes is assigned with the same number of devices. Moreover, we should mention that the presented results obtained by method UNI, COMB, and MSU for a particular traffic profile were the same regardless of the number of available transponders and results of UNI and COMB algorithms were even the same for different traffic profiles. These two facts directly follow from the design of these methods. Only the SAUR method accounts for the number of transponders; therefore, for SAUR we report results obtained for three analyzed values of available transponders denoted as SAUR(10,000), SAUR(15,000), and SAUR(20,000). Analyzing the results, we can observe how the tested methods had different strategies, as they assign the transponders to nodes in the network differently. In particular, the SAUR method tended to place more devices in network nodes in the center of the US (e.g., Dallas, Denver), especially for 20,000 transponders which allows to regenerate longer lightpaths (east coast–west coast traffic) and thus use more efficient modulation formats on shorter segments. In consequence, less transponder and spectrum resources were consumed which, in the end, made it possible to allocate more traffic. The largest differences among the analyzed methods can be observed for the traffic profile A (uniform traffic among all node pairs), while for traffic more dependent on the distance between end nodes (i.e., traffic profiles B and C) the differences among the analyzed methods are smaller. This can be explained by the fact that for traffic profiles B and C, there was more traffic between end nodes located closer and thus less transponders were required for regeneration.

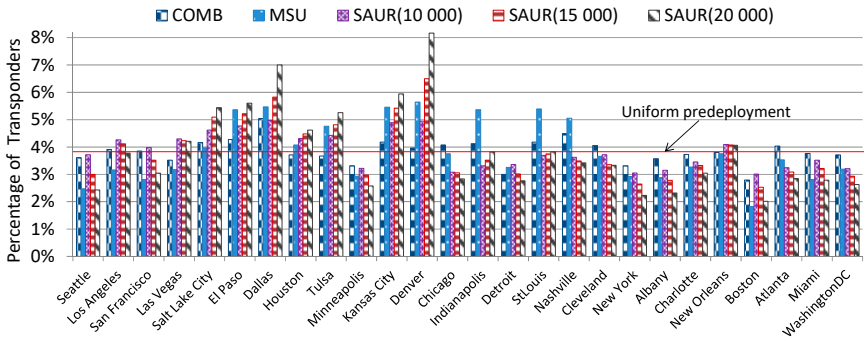

Figure 8. Placement of transponders in nodes of network US26 for traffic profile TP A as a function of various algorithms.

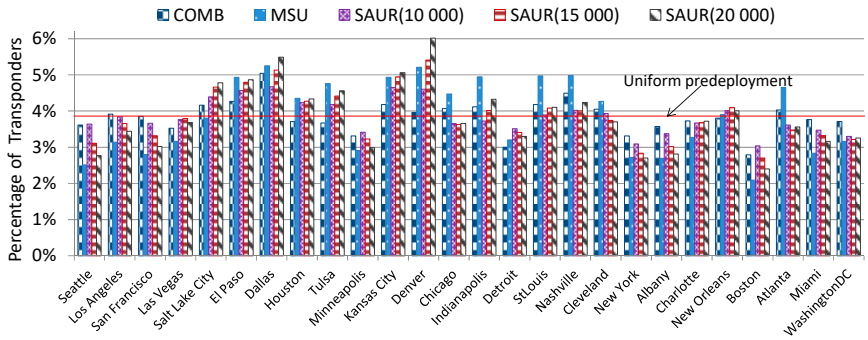

Figure 9. Placement of transponders in nodes of network US26 for traffic profile TP B as a function of various algorithms.

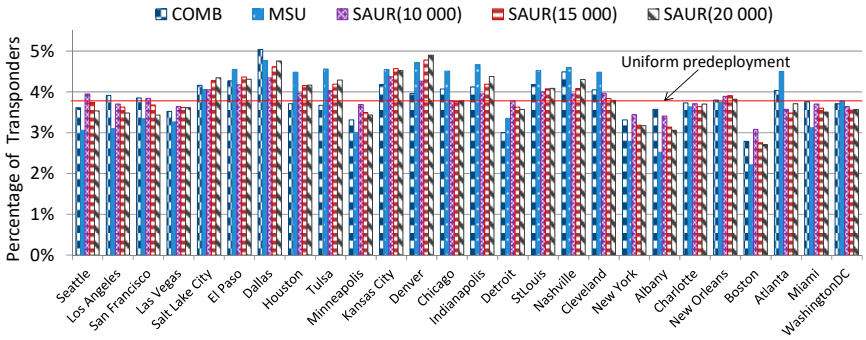

Figure 10. Placement of transponders in nodes of network US26 for traffic profile TP C as a function of various algorithms.

Moreover, it should be noted that SAUR placed much more transponders in some nodes when the budget was 20,000 devices compared to when the budget was 10,000 devices. The largest such differences were observed again for the traffic profile TPA and for nodes located in the center of the US. Once again it can be explained by the fact that with the larger budget of transponders, more regeneration points are possible (see Figures 11–13). These regeneration points are mostly used for longer lightpaths such as the east cost–west coast traffic which allows to change less spectral efficient modulation formats to more efficient modulation formats and thus consume less resources that can be next utilized for other lightpaths. Finally, more traffic can be accepted in the network.

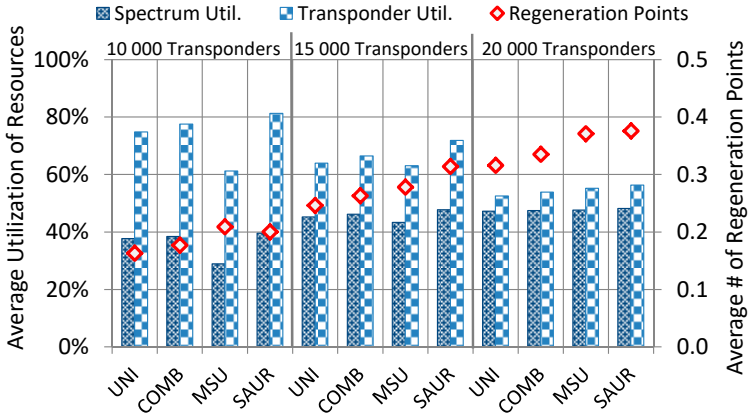

Figure 11. Utilization of spectrum and transponders and average number of regeneration points for the US26 network and TP A as a function of various algorithms and number of transponders.

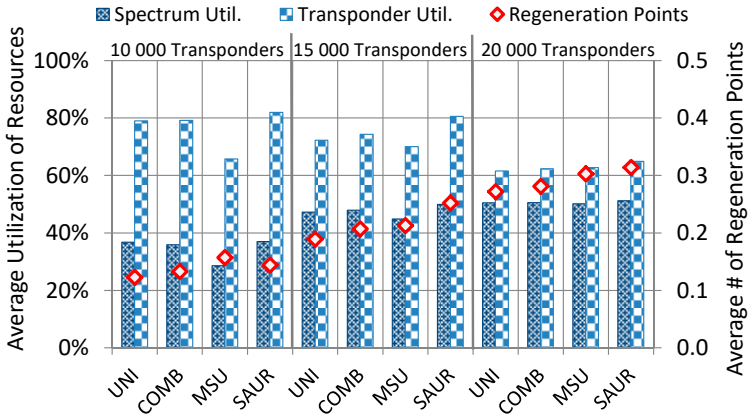

Figure 12. Utilization of spectrum and transponders and average number of regeneration points for the US26 network and TP B as a function of various algorithms and number of transponders.

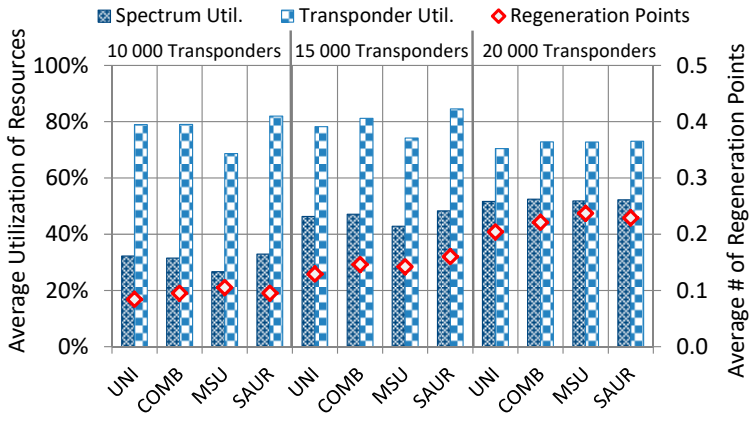

Figure 13. Utilization of spectrum and transponders and average number of regeneration points for the US26 network and TP C as a function of various algorithms and number of transponders.

In Figures 11–13, we report more detailed results for the same cases such as in Figures 8–10. Each figure shows the average results on utilization of spectrum and transponders (bars) and average number of regeneration points (points). The main observation is that in all cases, the SAUR method provided the best (highest) utilization of spectrum and transponders. In other words, the placement of transponders yielded by SAUR allowed to utilize the network resources to the highest extent which, in consequence, allowed to allocate more traffic than the other methods. In terms of the number of regeneration points (i.e., how many times on average the lightpath was regenerated), the SAUR and MSU methods experienced the highest values. Finally, both traffic profile and number of available transponders influenced the observed results; however, the impact was not very large.

We want to point out that the applied dynamic routing algorithm ARBR [11] used 5 candidate routing paths in the routing process and was able to efficiently adapt to the limited spectrum and transponder resources available in the network. In consequence, even when the transponders were not predeployed in an optimal way in the network, the algorithm itself can to a large extent improve the results of accepted traffic by adapting the routing and spectrum allocation process. However, even with such an intelligent dynamic routing method, the SAUR algorithm outperformed the other analyzed algorithms. Note that due to the limited space, we did not present detailed results of transponder placement for the Euro28 network; however, the obtained trends were comparable to those in the US26 network.

The last Figures 14–16 show more detailed results of two methods: UNI and SAUR for US26 network, 15,000 transponders, and traffic profiles: TP A, TP B, and TP C. Each graph shows the box plot of used transponders. The data were collected in every time iteration of the dynamic routing simulations. The dotted line shows the number of transponders predeployed in each node according to the results yielded by a particular algorithm. For the UNI method this value was constant (i.e., each node was assigned with the same number of transponders), while for the SAUR method, it was different for particular nodes. The red line represents the average observed values of transponder usage during the simulations (i.e., how many transponders were used for transmitting/receiving of optical signals at the source/destination nodes and regeneration of the signals at some intermediate nodes). In turn, the boxes show data on transponders' average usage through their quartiles. The presented figures clearly confirm that the SAUR method can utilize transponders much better than UNI. Moreover, the placement of transponders yielded by the SAUR method (limit of transponders) allowed more sustainable use in particular nodes, while for the UNI method some nodes used only a small part of available devices.

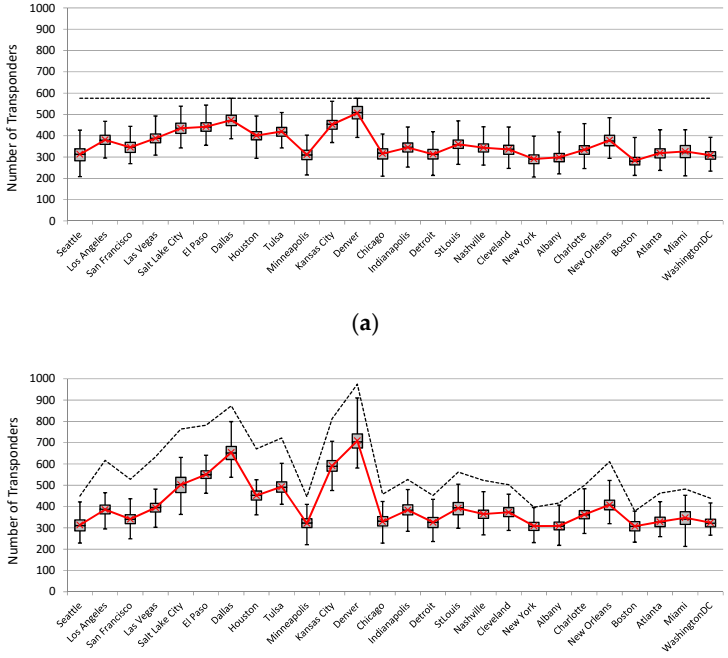

(**a**)

(**b**)

Figure 14. Box graph with placement of transponders given by: (**a**) UNI and (**b**) SAUR algorithms, for the US26 network, TP A, and 15,000 transponders. The dotted line shows the number of transponders in each node according to a particular algorithm. The red line represents the average observed values of transponder usage, while the boxes show data through their quartiles.

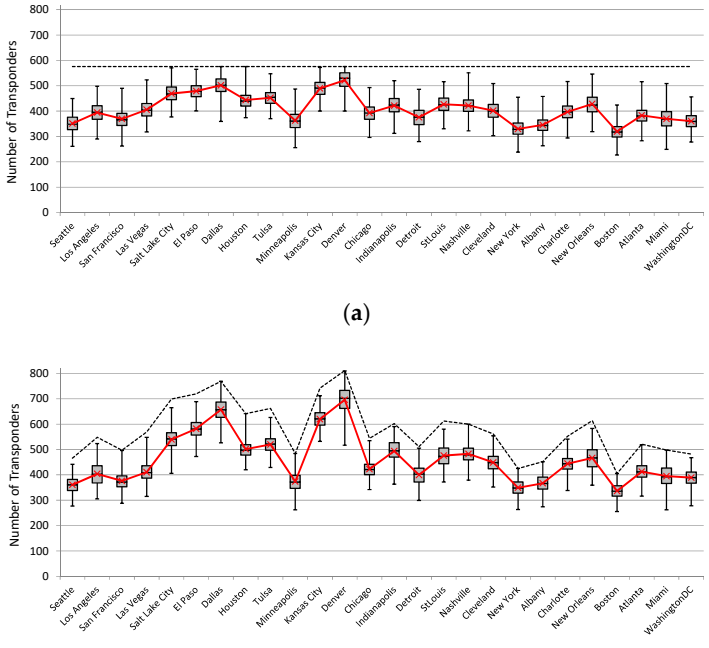

(**a**)

(**b**)

Figure 15. Box graph with placement of transponders given by: (**a**) UNI and (**b**) SAUR algorithms, for the US26 network, TP B, and 15,000 transponders. The dotted line shows the number of transponders in each node according to a particular algorithm. The red line represents the average observed values of transponder usage, while the boxes show data through their quartiles.

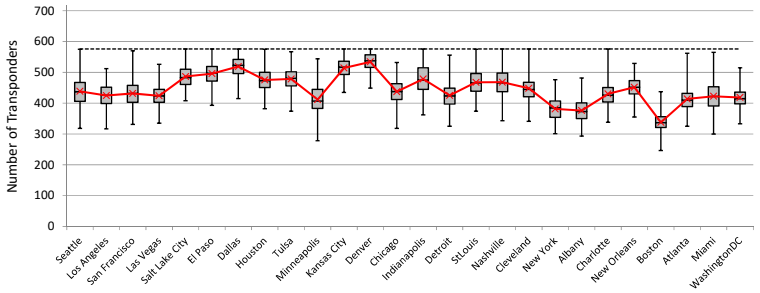

(**a**)

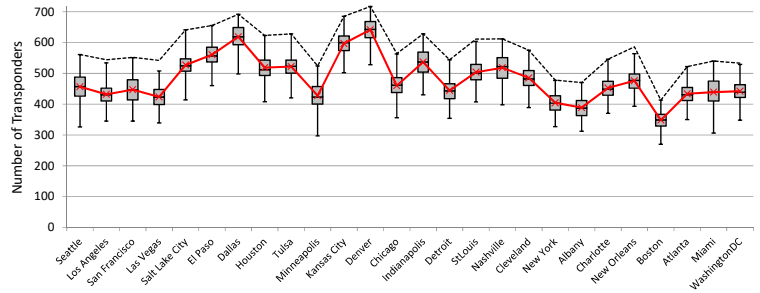

(**b**)

Figure 16. Box graph with placement of transponders given by: (**a**) UNI and (**b**) SAUR algorithms, for the US26 network, TP C, and 15,000 transponders. The dotted line shows the number of transponders in each node according to a particular algorithm. The red line represents the average observed values of transponder usage, while the boxes show data through their quartiles.

6. Conclusions

We have addressed the optimization problem of transponder predeployment in dynamic spectrally and spatially flexible optical networks in which the transponder resources are used both for transmitting/receiving (add/drop) spectral super-channels at source/destination nodes and for flexible super-channel regeneration in intermediate nodes which is achieved by means of the B2B regeneration approach. This problem consists in deciding on the number of transponders located in each network node, where the total number of transponders to be deployed in the network is limited. The problem was addressed under the consideration of multiple modulation formats, where each modulation format had specific spectral efficiency and transmission reach, and it was applied in accordance to the length of transparent segments that form translucent (regenerated) lightpaths. We showed that the decision on where the transponders are located has a significant impact on network performance, in particular, on the amount of accepted traffic. We proposed a heuristic method called scaled average used regenerators (SAUR) which makes use of a data analytics approach and decides on the transponder placement by exploiting information about network traffic characteristics and evaluated network performance. To assess the algorithm performance, we performed extensive simulation experiments on two representative network topologies and using several traffic profiles.

The main conclusions from this study are the following. Firstly, the SAUR algorithm provided much better performance results (in terms of accepted traffic) in all the evaluated network and traffic scenarios than the reference methods that were implemented and evaluated in this study. It is important to notice that an optimized placement of transponders in an SS-FON, which was achieved with SAUR, allows to increase the network throughput using only the existing resources, i.e., the network operator does not have to invest in new transponder devices or fibers to increase the served traffic and, in consequence, to increase the income.

The next conclusion is that the performance gaps between SAUR and the reference methods were larger for the US26 network than for the Euro28 network. It was due to the larger average distance between node pairs in US26 for which optimal placement of transponders is more beneficial since more spectrally efficient modulation formats than BPSK can be used and, therefore, savings in the spectrum usage can be achieved. Moreover, the SAUR method provided the best (highest) utilization of transmission resources (spectrum and transponders). In other words, the placement of transponders yielded by SAUR allowed to utilize the network resources to the highest extent which in consequence allowed to allocate more traffic than the other methods.

Furthermore, the proposed SAUR method can be used to estimate the number of transponders required in the network to serve a given amount of traffic. In particular, by running the SAUR method assuming different transponders' budgets (number of available transponders), we can obtain the estimated amount of traffic that can be provisioned in the network within a particular transponder budget. Next, by a simple comparison of the obtained values against the predicted network traffic, we can acquire the required number of transponders. This approach is valid for different traffic profiles. In consequence, a better placement of transponders provided by SAUR opens an opportunity to reduce the number of transponders required to serve a particular amount traffic in the network compared to other placement methods. This can also lead to a reduction in the energy consumption of the network.

In future work we will investigate the offline version of the optimization problem related to predeployment of transponders solved together with routing, space, and spectrum allocation in SS-FONs. Additionally, we plan to extend the study on the SS-FON scenarios in which multi-core fiber (MCF) links are used and the inter-core crosstalk effect that affects transmission quality is taken into account. Moreover, an interesting direction for future research is taking into account more accurate transmission reach models that would also include the type of equipment (e.g., optical amplifiers, reconfigurable optical add-drop multiplexers (ROADMs)) when considering the actual reach of the lightpaths with different modulation formats and with the use of the Gaussian noise (GN) model for accurate OSNR (optical-signal-to-noise Ratio) estimation in nonlinear fiber propagation.

Author Contributions: Conceptualization, K.W., M.K., A.K.; methodology, K.W., M.K, A.K.; software, K.W., A.W.; investigation, experiments, input data, K.W., A.W.; writing—original draft preparation, K.W., M.K., A.W., A.K.; writing—review and editing, K.W., M.K., A.W., A.K.; supervision, K.W.; project administration, K.W., M.K.; funding acquisition, K.W., M.K. All authors have read and agreed to the published version of the manuscript.

Funding: The work of K. and A.W. was supported by the National Science Centre, Poland, under Grant 2017/27/B/ST7/00888. The work of M.K. was supported by the National Science Centre, Poland, under Grant 2016/21/B/ST7/02212.

Conflicts of Interest: The authors declare no conflict of interest.

References

1. Klonidis, D.; Cugini, F.; Gerstel, O.; Jinno, M.; Lopez, V.; Palkopoulou, E. Spectrally and spatially flexible optical network planning and operations. *IEEE Commun. Mag.* **2015**, *53*, 69–78. [CrossRef]
2. Marom, D.M.; Colbourne, P.D.; D'errico, A.; Fontaine, N.K.; Ikuma, Y.; Proietti, R. Survey of photonic switching architectures and technologies in support of spatially and spectrally flexible optical networking [invited]. *IEEE Osa J. Opt. Commun. Netw.* **2017**, *9*, 1–26. [CrossRef]
3. Klinkowski, M.; Lechowicz, P.; Walkowiak, K. Survey of resource allocation schemes and algorithms in spectrally-spatially flexible optical networking. *Opt. Switch. Netw.* **2018**, *27*, 58–78. [CrossRef]
4. Shen, G.; Tucker, R.S. Translucent optical networks: The way forward. *IEEE Commun. Mag.* **2007**, *45*, 48–54. [CrossRef]
5. Walkowiak, K. *Modeling and Optimization of Cloud-Ready and Content-Oriented Networks*; Studies in Systems, Decision and Control; Springer: Berlin/Heidelberg, Germany, 2016; Volume 56.
6. Eira, A.; Santos, J.; Pedro, J.; Pires, J. Multi-objective design of survivable flexible-grid DWDM networks. *IEEE Osa J. Opt. Commun. Netw.* **2014**, *6*, 326–339. [CrossRef]

7. Fallahpour, A.; Beyranvand, H.; Nezamalhosseini, S.A.; Salehi, J.A. Energy efficient routing and spectrum assignment with regenerator placement in elastic optical networks. *J. Lightwave Technol.* **2014**, *32*, 2019–2027. [CrossRef]
8. Klinkowski, M.; Walkowiak, K. On performance gains of flexible regeneration and modulation conversion in translucent elastic optical networks with super-channel transmission. *J. Lightwave Technol.* **2016**, *34*, 5485–5495. [CrossRef]
9. Zami, T.; Morea, A.; Pesic, J. Benefit of progressive deployment of regenerators along with traffic growth in WDM elastic networks. In Proceedings of the Optical Fiber Communication Conference OFC, Tu2F.3, San Diego, CA, USA, 11–15 March 2018.
10. Morea, A.; Zami, T. Optimized Regenerator Placement in Elastic Optical Networks. In Proceedings of the 2017 European Conference on Optical Communication (ECOC), Gothenburg, Sweden, 17–21 September 2017.
11. Walkowiak, K.; Lechowicz, P.; Klinkowski, M. Dynamic Routing in Spectrally-Spatially Flexible Optical Networks with Back-to-Back Regeneration. *IEEE/Osa J. Opt. Commun. Netw.* **2018**, *10*, 523–534. [CrossRef]
12. Walkowiak, K.; Klinkowski, M. Predeployment of Transceivers for Dynamic Lightpath Provisioning in Translucent Flexgrid Optical Networks. In Proceedings of the Optical Fiber Communications Conference and Exhibition (OFC), San Diego, CA, USA, 11–15 March 2018.
13. Chen, S.; Ljubic, I.; Raghavan, S. The regenerator location problem. *Networks* **2010**, *55*, 205–220. [CrossRef]
14. Yang, X.; Ramamurthy, B. Sparse regeneration in translucent wavelength-routed optical networks: Architecture, network design and wavelength routing. *Photonic Netw. Commun.* **2005**, *10*, 39–53. [CrossRef]
15. Garcia-Manrubia, B.; Pavon-Marino, P.; Aparicio-Pardo, R.; Klinkowski, M.; Careglio, D. Offline Impairment-Aware RWA and Regenerator Placement in Translucent Optical Networks. *J. Lightwave Technol.* **2011**, *29*, 265–277. [CrossRef]
16. Flammini, M.; Marchetti-Spaccamela, A.; Monaco, G.; Moscardelli, L.; Zaks, S. On the Complexity of the Regenerator Placement Problem in Optical Networks. *IEEE Acm Trans. Netw.* **2011**, *19*, 498–511. [CrossRef]
17. Chaves, D.A.; Carvalho, R.V.; Pereira, H.A.; Bastos-Filho, C.J.; Martins-Filho, J.F. Novel strategies for sparse regenerator placement in translucent optical networks. *Photonic Netw. Commun.* **2012**, *24*, 237–251. [CrossRef]
18. Pedro, J. Predeployment of regenerators for fast service provisioning in DWDM transport networks. *IEEE/Osa J. Opt. Commun. Netw.* **2015**, *7*, A190–A199. [CrossRef]
19. Klinkowski, M. On the effect of regenerator placement on spectrum usage in translucent Elastic Optical Networks. In Proceedings of the 14th International Conference on Transparent Optical Networks ICTON, Coventry, UK, 2–5 July 2012; pp. 1–6.
20. Nag, A.; Tornatore, M.; Mukherjee, B. On the effect of channel spacing, launch power, and regenerator placement on the design of mixed-line-rate optical networks. *Opt. Switch. Netw.* **2013**, *10*, 301–311. [CrossRef]
21. Aibin, M.; Walkowiak, K. Regenerator placement algorithms for cloud-ready Elastic Optical Networks. In Proceedings of the 17th International Conference on Transparent Optical Networks ICTON, Budapest, Hungary, 5–9 July 2015; pp. 1–4.
22. Madani, F.M. Scalable Framework for Translucent Elastic Optical Network Planning. *J. Lightwave Technol.* **2016**, *34*, 1086–1097. [CrossRef]
23. Brasileiro, Í.; Valdemir, J.; Soares, A. Regenerator Assignment with circuit invigorating. *Opt. Switch. Netw.* **2019**, *34*, 58–66. [CrossRef]
24. Cavalcante, M.A.; Pereira, H.A.; Chaves, D.A.R.; Almeida, R.C., Jr. An auxiliary-graph-based methodology for regenerator assignment problem optimization in translucent elastic optical networks. *Opt. Fiber Technol.* **2019**, *53*, 102008. [CrossRef]
25. da Silva, E.F.; Almeida, R.C.; Pereira, H.A.; Chaves, D.A. Assessment of novel regenerator assignment strategies in dynamic translucent elastic optical networks. *Photonic Netw. Commun.* **2020**, *39*, 54–69. [CrossRef]
26. Rottondi, C.; Boffi, P.; Martelli, P.; Tornatore, M. Routing, modulation format, baud rate and spectrum allocation in optical metro rings with flexible grid and few-mode transmission. *J. Lightwave Technol.* **2017**, *35*, 61–70. [CrossRef]
27. Khodashenas, P.S.; Rivas-Moscoso, J.M.; Siracusa, D.; Pederzolli, F.; Shariati, B.; Klonidis, D. Comparison of spectral and spatial super-channel allocation schemes for SDM networks. *J. Lightwave Technol.* **2016**, *34*, 2710–2716. [CrossRef]

28. Walkowiak, K.; Klinkowski, M.; Lechowicz, P. Scalability Analysis of Spectrally-Spatially Flexible Optical Networks with Back-to-Back Regeneration. In Proceedings of the 20th International Conference on Transparent Optical Networks ICTON, Bucharest, Romania, 1–5 July 2018.
29. Christodoulopoulos, K.; Soumplis, P.; Varvarigos, E. Planning flexible optical networks under physical layer constraints. *IEEE Osa J. Opt. Commun. Netw.* **2013**, *5*, 1296–1312. [CrossRef]
30. Orlowski, S.; Pióro, M.; Tomaszewski, A.; Wessäly, R. SNDlib 1.0—Survivable network design library. Proceedings of the 3rd International Network Optimization Conference INOC 2007. Available online: http://sndlib.zib.de (accessed on 1 February 2019).
31. Deore, A.; Turkcu, O.; Ahuja, S.; Hand, S.J.; Melle, S. Total cost of ownership of WDM and switching architectures for next-generation 100Gb/s networks. *IEEE Commun. Mag.* **2012**, *50*, 179–187. [CrossRef]